The EMBO Journal vol.5 no.6 pp.1395-1402, 1986

Cryo-electron microscopy of vitrified chromosomes *in situ*

A.W.McDowall, J.M.Smith and J.Dubochet

European Molecular Biology Laboratory (EMBL), Postfach 10.2209, D-6900 Heidelberg, FRG

Communicated by J.-E.Edstrom

Chromosomes of metaphase-arrested Chinese hamster ovary (CHO) and HeLa cells were examined *in situ*, unfixed and unstained, by cryo-electron microscopy. In hydrated, vitrified cryo-sections, chromosomes exhibit a characteristic homogeneous, grainy texture, which, on optical diffraction, gives rise to a broad reflection corresponding to 11 nm. No superstructure or periodic order is discernible. These observations suggest that the chromosome is formed by the compact association of 11 nm filaments, or portions thereof, interacting in a manner akin to the molecules of a liquid. Some implications of the liquid model of chromosome structure are discussed.

Key words: chromosome/HeLa cell/CHO cell/cryo-electron microscopy/mitotic chromosome

Introduction

The metaphase chromosome is a condensed form of chromatin. It consists of two apparently identical chromatids, each formed by the association of a long DNA molecule with an approximately equal mass of histones and a variable amount of non-histone protein (Bostock and Sumner, 1978). Within this structure, the duplicated DNA must be packaged in a form that allows the orderly segregation of the chromatids. The accepted view is that the organization of the chromosome, and chromatin in general, is made at several levels. The first level forms the nucleosomes, each of which consists of 146 bp of DNA associated with an octamer of histones (Klug and Butler, 1983). It has been proposed that strings of nucleosomes are wound into a higher order structure, variously suggested to consist of a series of beads (Jorcano *et al.*, 1980), a continuous solenoid (Finch and Klug, 1976; Klug and Butler, 1983; Widom and Klug, 1985) or a helical ribbon (Woodcock *et al.*, 1984). These structures may, in turn, form loops, and a non-histone protein scaffold could arrange these loops along the chromosome (Paulson and Laemmli, 1977; Butler, 1983).

Models of the higher levels of chromatin structure have been based principally upon data obtained by small-angle diffraction of X-rays (e.g. Langmore and Paulson, 1983) and neutrons (e.g. Bram *et al.*, 1977), or by electron microscopy (e.g. Rattner and Hamkalo, 1978). These methods all have their limitations. Diffraction is a function of the scattering properties of the entire specimen, and since chromatin constitutes only a small part of the cell, it must be isolated in order to obtain unambiguous diffractograms. Although much effort has been devoted towards the development of non-disruptive isolation procedures, there is still uncertainty as to whether the material from which well-defined diffractograms can be obtained is a faithful representation of the *in vivo* state. In addition, native chromatin is relatively poorly ordered, and diffractograms are difficult to interpret. Electron microscopy has the advantage of providing a direct image of chromatin *in situ*. Its usefulness is impaired, however, by various preparative artefacts arising when the native, hydrated structure is transformed into the rigid block required for conventional thin sectioning. Here also, there is considerable uncertainty as to whether the features observed faithfully represent chromatin *in vivo*.

The newly-developed technique of cryo-electron microscopy of vitrified sections combines the advantages of direct imaging whilst avoiding the artefacts produced by conventional plastic embedding (McDowall *et al.*, 1983; Dubochet *et al.*, 1983). Specimens are cooled sufficienty rapidly to prevent formation of ice crystals, and sections are cut and imaged at low temperature to avoid sublimation of water. Image resolution is comparable with that obtained using conventional procedures (McDowall *et al.*, 1984). In the present work we have used this technique to study the structure of metaphase chromosomes *in situ* in vitrified, unfixed and unstained Chinese hamster ovary (CHO) and HeLa cells.

Results

Chromosomes in metaphase-arrested HeLa and CHO cells, incubated in the sucrose-containing medium required for vitrification, appear normal by optical microscopy and by electron microscopy of conventionally fixed and embedded samples. By optical fluorescence microscopy, chromosomes of intact cells stained with acridine orange or 4,6-diamidino-2-phenylindole (DAPI) are indistinguishable in appearance and distribution from those of control cells which have not been exposed to 20% sucrose (not shown). In Epon sections stained with uranium and lead, chromosomes exhibit the usual appearance of large, irregular electron-dense regions with a convoluted outline (Figure 1a). At higher magnification, the internal structure of the chromosome appears as a coarse, uneven distribution of stain (Figure 1b). Optical diffraction reveals a well-defined circle corresponding to a spacing of ~7 nm (Figure 1b, insert).

Optical microscopy demonstrates that the average cell diameter shrinks, typically from ~20 to 16 μm, in response to the osmotic effect of sucrose. The density of the cytosol is increased accordingly, thus reducing the contrast of unstained chromosomes observed by phase and Nomarski interference contrast. Despite this shrinkage, cells remain viable, as evidenced by their ability to exclude trypan blue and grow normally on resuspension in sucrose-free medium (not shown).

Images of vitrified, unstained sections of intact cells are characterized by a good representation of fine structure, low overall contrast and severe cutting artefacts (Figure 2a). The quality of the fine structure representation depends sharply on the thickness of the section; the best are ~70 nm thick and image quality becomes poor when thickness exceeds 200 nm. The sections must also be free from severe water contamination.

Contrast can be improved by freeze-drying the section in the electron microscope (Figure 2b). Organelles then become easily

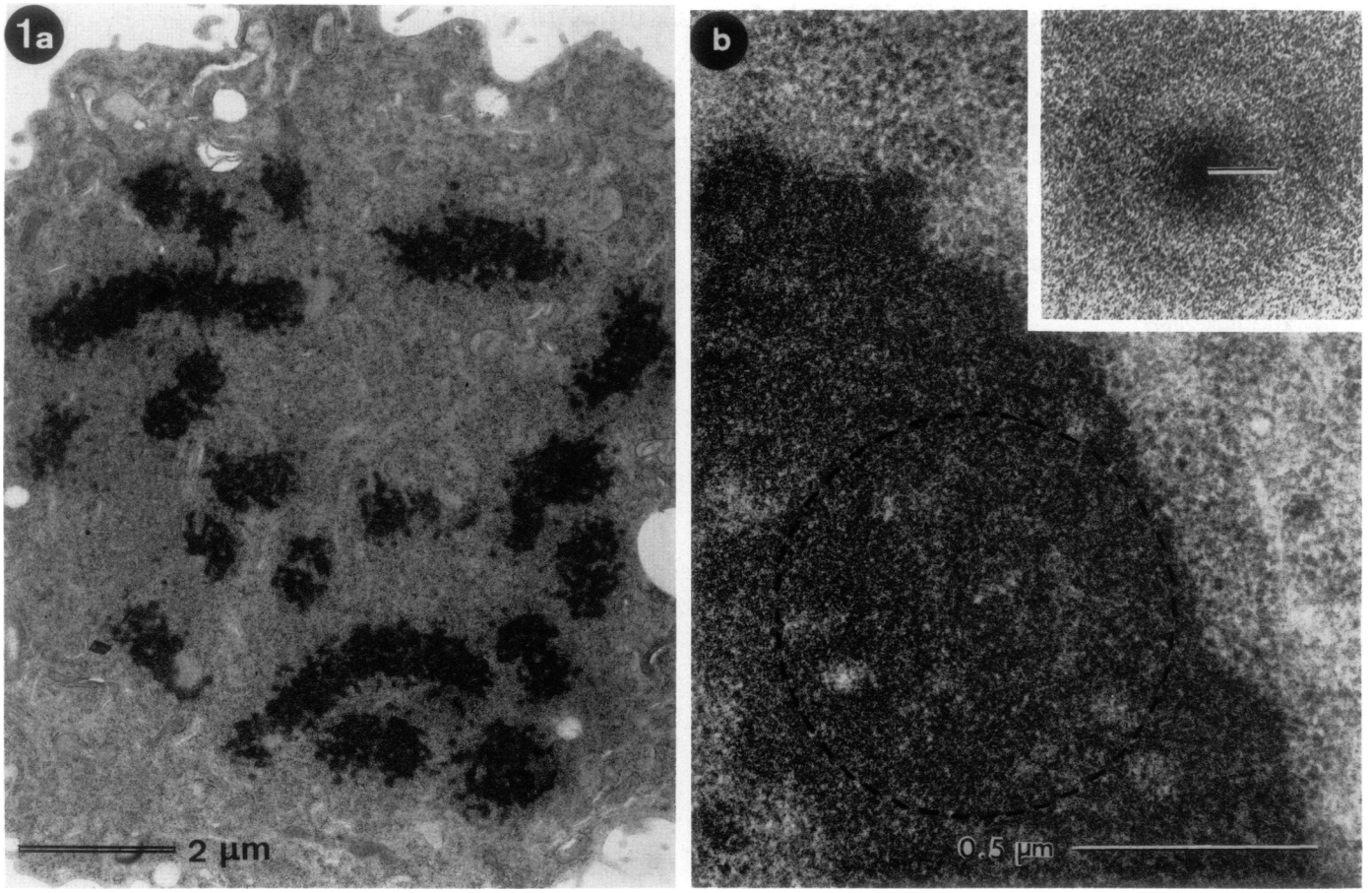

Fig. 1. Metaphase-arrested CHO cells conventionally fixed and Epon-embedded. **(a)** Survey micrograph of cell grown in medium containing 20% sucrose, the same solution that was used for freezing. Magnification: 11 000×. **(b)** High magnification image of part of a chromosome from a cell grown in normal (sucrose-free) medium. Magnification: 66 000×. **Insert:** optical diffractogram from circled region. The bar corresponds to a spacing of 10 nm.

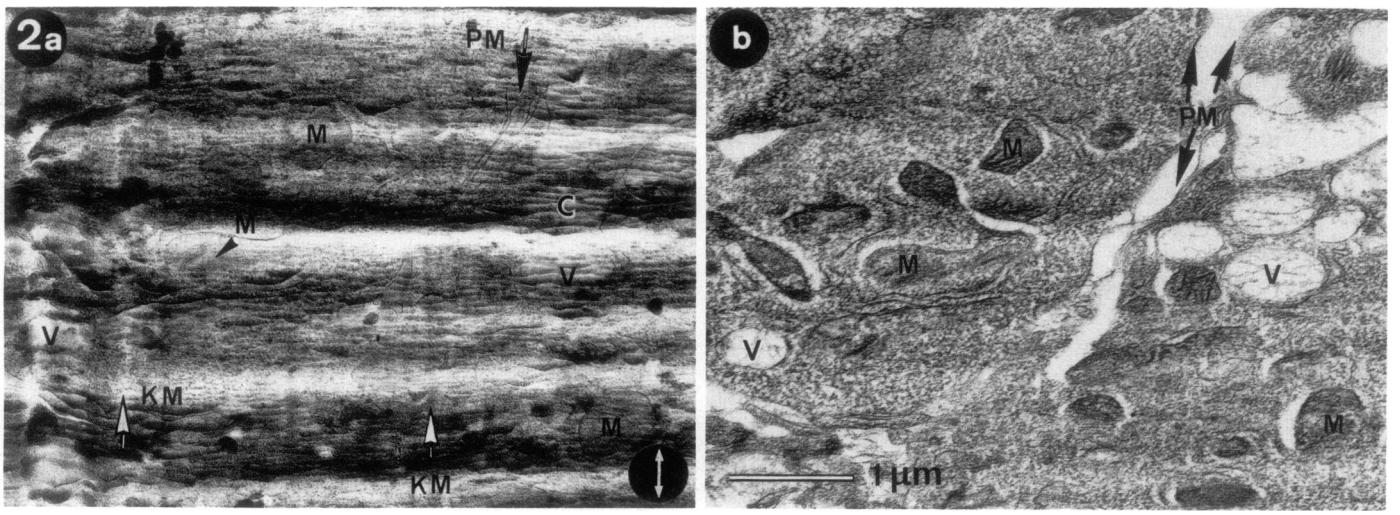

Fig. 2. Interphase HeLa cells. **(a)** Hydrated, vitrified section of average quality, **(b)** same area after freeze-drying in the electron microscope. The cutting direction is marked by a circled arrow. PM: plasma membranes; M: mitochondria; V: vesicles; KM: knife marks; C: crevasses. Thickness: 120 nm. Magnification: 16 500×.

visible, but resolution is lost. It is preferable, therefore, to record images of the fully hydrated state, though they require more careful inspection than micrographs of freeze-dried or conventional preparations. Freeze-drying is, nevertheless, useful because it permits calculation of the hydration of the cell (Dubochet *et al.*, 1983). The average dry-mass fraction of the cell was found to be 29 ± 5% by this method.

Cutting artefacts are of three major types: chatter, knife marks

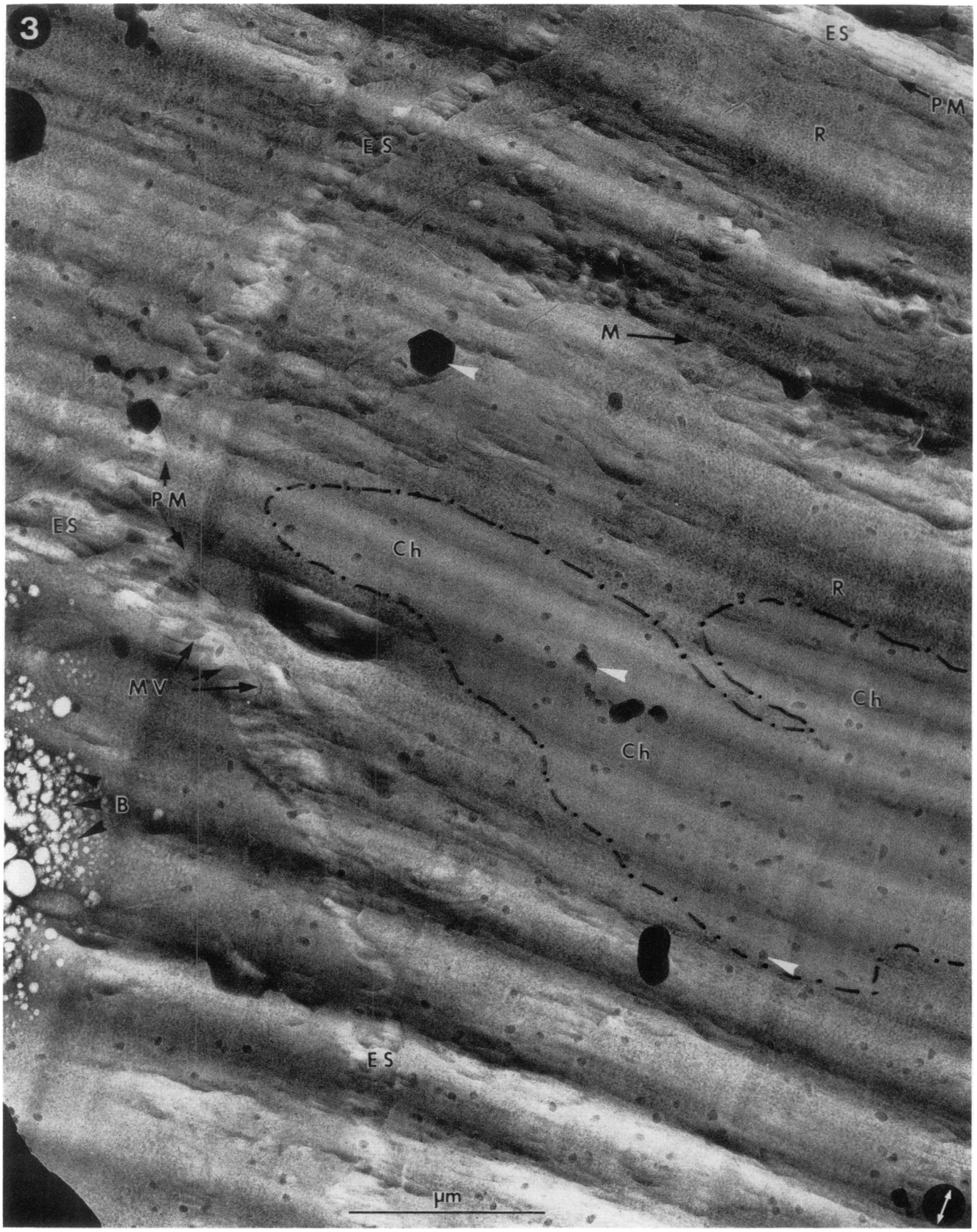

Fig. 3. Survey micrograph of a hydrated, vitrified section of metaphase-arrested CHO cells. Regions of three cells are discernible against the less dense extracellular space (ES). Cellular structures depicted include: plasma membrane (PM); mitochondria (M); ribosomes (R); and microvilli (MV). A large chromosomal region (Ch), free of ribosomes and other organelles, is outlined. Beam-induced bubbling (B) and water contamination (white arrow heads) are also apparent. Circled arrow indicates cutting direction. Underfocus: 4 μm. Magnification: 35 000×.

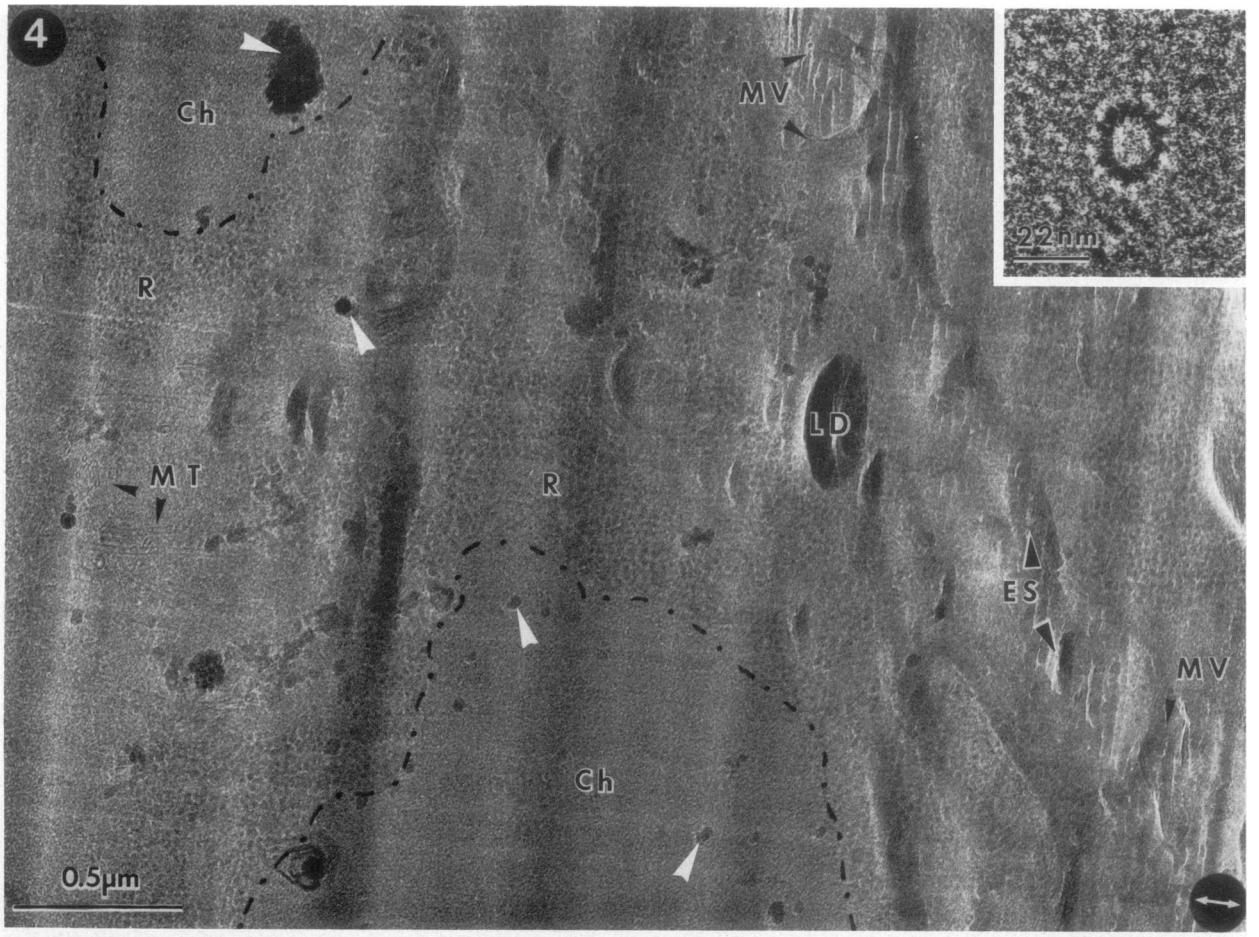
4
Ch
MV
R
LD
MT
R
ES
MV
Ch
0.5μm
22nm

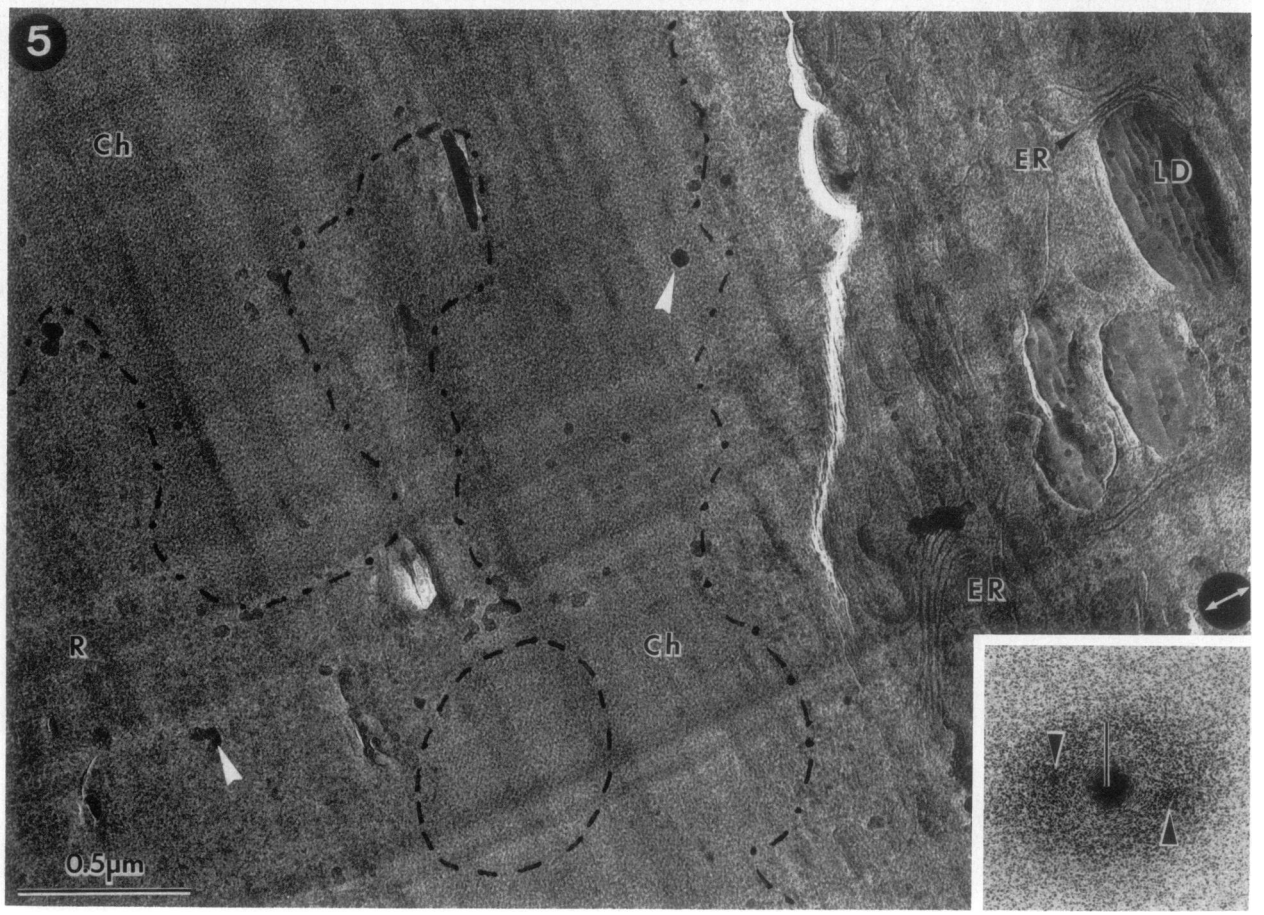
5
Ch
ER
LD
ER
R
Ch
0.5μm

and 'crevasses' (Chang *et al.*, 1983). As can be seen from the elliptical appearance of lipid droplets (e.g. Figure 4a) sections are also compressed by 25 – 50% along the cutting direction. As a result of these technical limitations, and the small dimensions of the vitrified volume, it is difficult to obtain large, high-quality vitrified sections routinely.

The general appearance of vitrified metaphase-arrested cells is shown in Figures 3 – 5. The outline of the cell is discernible against the low-density extracellular space. Furthermore, the extracellular space is more prone to fracture and consequently contains a conspicuous network of crevasses. The cell interior exhibits many characteristic structures. Membranes are visible when their plane is approximately parallel to the viewing direction. Lipid droplets and membranous organelles such as the plasma membrane, endoplasmic reticulum and mitochondria, are recognizable. Components of the cytoskeleton can be seen in most sections. For example, microtubules are discernible, even if they are in the plane of the section (Figure 4). When oriented along the viewing axis, individual protofilaments can be distinguished (Figure 4, insert). Most of the cell volume contains large amounts of ribosomes, forming an homogeneous population of ~30 nm sized bodies.

Chromosomes are easily recognized because they are the only sizeable regions free of ribosomes and other organelles. They have the size and distribution expected from conventional electron microscopy. Their outline is, however, smoother than in most conventional preparations and the boundary between adjacent chromosomes is frequently indiscernible. Chromosomes are also recognized by their grainy, homogeneous texture (Figures 5 and 6). It is best characterized in the optical diffractogram of the thinnest speicmens where it gives rise to a broad ellipse, with small axis corresponding to a spacing of 11 ± 1 nm, surrounding a central low density region (Figure 6, insert a). The long axis of the ellipse is always parallel to the cutting direction, demonstrating that the elliptical shape of the diffractogram is a consequence of compression during sectioning, and that the grainy texture is not an optical artefact. This latter point is confirmed by the observation that the size of the ellipse is identical for two mirographs recorded from the same region but with different focus (not shown). In some regions of chromosome images the grainy texture is anisotropic (Figure 5, circled). It appears then as the very noisy image of bundles of parallel filaments. The preferential orientation of the grain is best revealed in the optical diffractogram, where one direction of the ellipse is reinforced (Figure 5, insert). The grainy texture appears much attenuated in thicker sections, where chromosomes seem nearly structureless.

The grainy texture described above is characteristic for hydrated, vitrified chromosomes observed *in situ*. It is found in no other region of the mitotic cell. In particular, the optical diffractogram of the ribosomal area shows neither the characteristic ellipse nor the central low density region (Figure 6, insert b). The chromosomes observed in conventionally embedded sections also lack this grainy texture.

Discussion

Cryo-electron microscopy of vitrified sections

Cryo-electron microscopy of vitrified sections allows observation of cellular ultrastructure in the hydrated state, and avoids the artefacts produced by conventional chemical fixation, embedding and staining. All the evidence presented to date shows that vitrification preserves the original biological structure, at least at the resolution considered in the present study (McDowall *et al.*, 1984; Lepault *et al.*, 1985). The method carries its own limitations, however, which arise from three main sources, namely: the necessity to achieve vitrification; the process of cryo-sectioning and the low inherent contrast of unstained hydrated specimens.

In the present study, vitrification was easily and reproducibly achieved by adding 20% sucrose to the normal growth medium. Although cells remain viable, the osmotic effect of 20% sucrose causes them to shrink to about half their normal volume. The concentration of the cytosol is expected to increase accordingly, and hydration measurements of vitrified sections do indeed show that the proportion of dry mass has the unusually high value of ~30%. As a result, the overall contrast of the chromosomes is reduced. This osmotic effect is less severe when using high mol. wt dextran as cyroprotectant, instead of sucrose. This advantage has to be paid for, however, by conferring upon the vitrified sample less favourable sectioning properties, and in particular by making sections more prone to the formation of crevasses. Nevertheless, preliminary experiments with dextran (not shown) confirm that the overall shape and characteristic grainy texture of the chromosome are not due to the effect of sucrose.

The process of cryo-sectioning imposes three major limitations. Firstly, resolution is limited by the mass thickness of the section. In practice, resolution much better than 10 nm is difficult to achieve (McDowall *et al.*, 1983). In this study, therefore, we consider only structures larger than this dimension. Secondly, it is difficult to obtain sections sufficiently large and regular to depict an entire cell, and much more so, to observe a cell population on a single section. Consequently, the overall apsect of a cell or the distribution of organelles in it must be deduced from the observation of many sections. Thirdly, all sections suffer from severe cutting artefacts. Fortunately, these artefacts are not such a severe limitation as might be thought from a superficial look at the sections. In most sections, there are relatively artefact-free regions. Furthermore, any transformations resulting from the cutting process itself are related to the cutting direction and can therefore always be recognized as such.

The unusually large degree of underfocus used to record images of unstained, vitrified specimens has been discussed previously (Lepault and Pitt, 1984; Adrian *et al.*, 1984). This requirement derives from the fact that, even for structures ~10 nm in size, imaging relies mostly on phase contrast, and not on amplitude contrast as in conventionally stained specimens. Nevertheless, for all micrographs presented here, the first zero of the transfer function is well outside the position correspon-

Fig. 4 and **5**. Hydrated, vitrified sections of metaphase-arrested CHO and HeLa cells, respectively. Chromosomes are indicated by dashed lines. The cutting direction is marked by a circled arrow. White arrow heads indicate contaminating ice crystals on the surface of the section. Ch: chromosome; LD: lipid droplets; MV: microvilli; MT: microtubules; R: ribosomes; ER: endoplasmic reticulum. In **Figure 4**, parts of two cells are visible, separated by the crevassed extracellular space (ES). Thickness: 170 nm. Underfocus: >10 μm. Magnification: 45 600×. **Insert:** enlarged view of a microtubule seen along its axis (from another micrograph of the same specimen). The ellipticity is due to compression during cutting. Thickness: 100 nm. Underfocus: 4.8 μm. Magnification: 455 000×. In **Figure 5**, parallel lines are faintly discernible in the circled region. Magnification: 46 800×. **Insert:** optical diffractogram of the circled region. Thickness: 86 nm. Underfocus: 6.6 μm. The reflections due to the parallel lines are indicated by the arrow heads. The bar corresponds to a spacing of 10 nm.

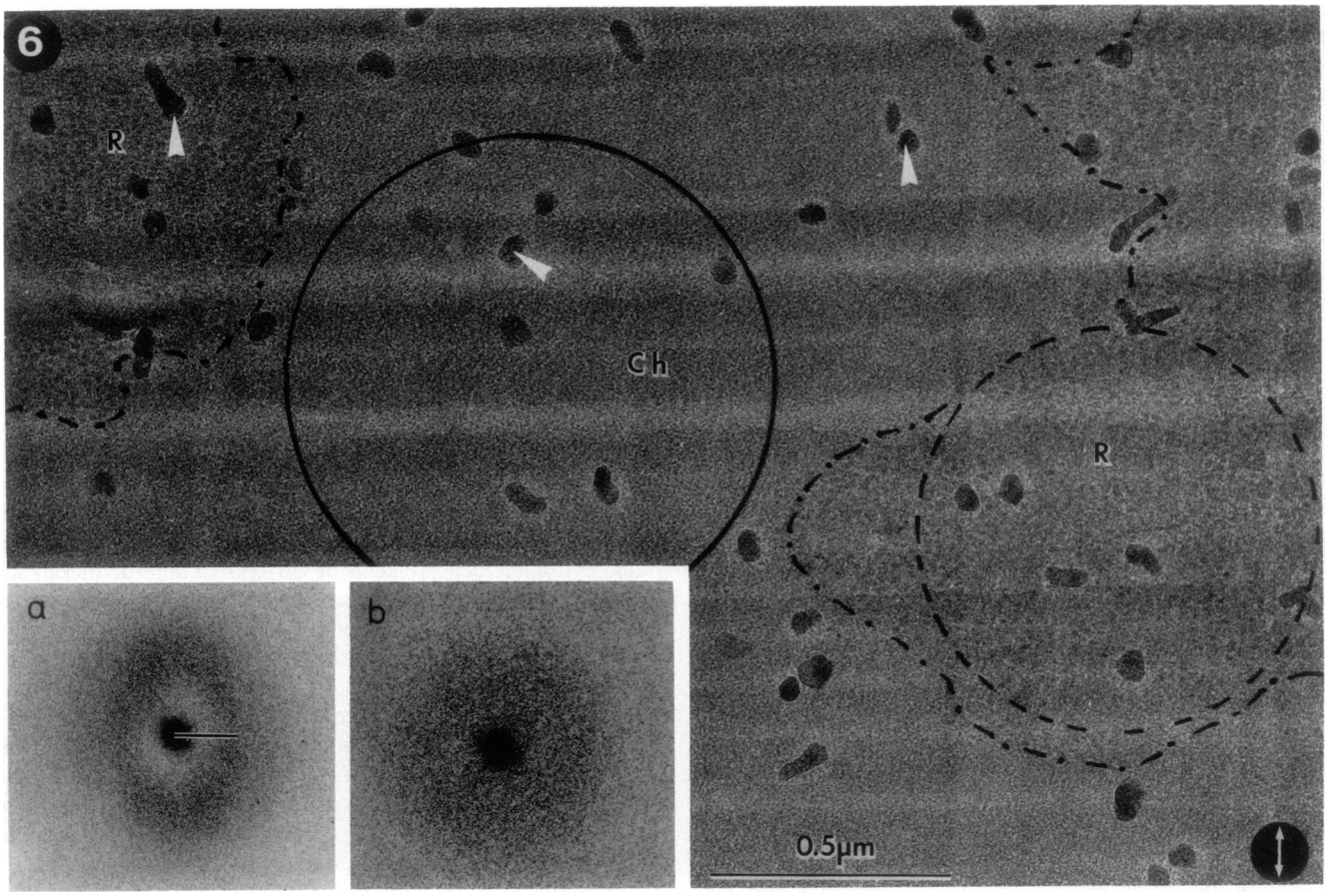

Fig. 6. Hydrated, vitrified section of a metaphase-arrested CHO cell, with a chromosomal region (Ch) outlined. Contaminating water is indicated by white arrow heads, and the circled arrow indicates cutting direction. Ribosomal regions adjacent to the chromosome are indicated (R). Thickness: 100 nm. Underfocus: 4.8 μm. Magnification: 65 000×. **Inserts:** optical diffractograms of **(a)** the region of the chromosome marked by the solid black circle, and **(b)** the region of the cytoplasm marked by the broken black circle. The bar corresponds to a spacing of 10 nm.

ding to the smallest structure considered. Contrast inversion is therefore excluded.

From the above we conclude that the images presented here of hydrated, vitrified chromosomes *in situ* reliably depict their structure *in vivo*.

Chromosome structure

The image of the vitrified chromosome has a characteristic homogeneous grainy texture, which gives rise, in thin sections, to an equally characteristic optical diffractogram. This texture is remarkable because it can be observed everywhere, in every chromosome, but it is not observed anywhere else in the mitotic cell. The only variation sometimes observed is the noisy image of parallel 11 nm filaments appearing in regions where the texture is anisotropic. Furthermore, the texture is observed only in vitrified specimens. In contrast, conventionally embedded chromosomes exhibit a comparatively irregular structure. They lack the 11 nm texture but show a preferential 7 nm spacing in optical diffraction. It is possible, therefore, that the 11 nm texture corresponds to the ~11 nm peak observed in many X-ray diffraction studies of chromatin (e.g. Langmore and Paulson, 1983). Its replacement by a 7 nm peak following dehydration has also been observed (Langmore and Schutt, 1980).

With regard to the structure of the chromosome, the grainy texture implies only that the 11 nm spacing corresponds to the dominant feature of its organization, and that there is no larger arrangement which is compact and massive enough to be depicted on the micrograph. This information is sufficient to draw some conclusions as to what the structure of the chromosome cannot be.

Firstly, the feature giving rise to the 11 nm texture cannot be organized into large, periodic structures. Any such structures, much larger than the section thickness, would be observable in the image. The local anisotropy frequently observed in the thinnest sections suggests, however, that some kind of partial order could extend over a long distance.

Secondly, the micrographs of vitrified sections show that, elsewhere in the cell, particles as small as ribosomes are easily visible. Larger compact and well separated particles, as could be superbeads (Jorcano *et al.*, 1980) or straight solenoids (Finch and Klug, 1976) should therefore be easily visible in the chromosome. The latter structures, for example, are thought to have a diameter of 30 nm and a mass per unit length of at least 130 kd/nm. These values are close to those of the microtubules (25 nm in diameter and 150 kd/nm), and we see in Figure 3 that microtubules are unmistakably visible in the section.

The grainy texture observed on the chromosome is, however, insufficient to deduce the precise origin of the 11 nm spacing, or, still less, to reconstruct the structure of the chromosome. Many possible models are compatible with our observations. For example, small supranucleosomal aggregates, as for example, those containing only about eight nucleosomes (Zentgraf and Franke, 1984) could be too small to be detected in the section. The same could hold for solenoids or helical structures if they are strongly fluctuating and intertwined.

However, the simplest model that can account for the 11 nm homogeneous texture only states that the chromosome is made by the disordered aggregation of ~11 nm subunits. In other words, the model states that the interaction between the subunits is not strong enough to define uniquely their position with respect to the others. Several discrete conformations — or a continuous range of conformations — are accessible within the thermal energy available in the system. The degree of freedom that the particles have, one with respect to the other, implies that they also have some degree of mobility. Structural order cannot extend over a long distance nor last for a long period of time. By definition the model implies that the 11 nm subunits are arranged in a way similar to that of the molecules in a liquid.

The nature of the subunits cannot be inferred from the observations presented here. However, it is known that the chromosome is made of nucleosomes (Compton *et al.*, 1976) and that nucleosome cores have a tendency to stack on top of each other into an 11 nm filament (Finch *et al.*, 1977; Dubochet and Noll, 1978). We propose therefore that the basic structure of the chromosome is that of a liquid-like compact aggregation of 11 nm filament portions. The anisotropy observed in some chromosomes would represent a local, partial alignment of the filaments. This liquid model is also the one we have deduced from observations of minichromosomes of SV40 (Dubochet *et al.*, 1986). It bears analogy with a proposal of Davies and Small (1968).

The liquid model is partially compatible with other models proposed previously. The superbead (Jorcano *et al.*, 1980; Zentgraf and Franke, 1984) is thought to be a compact but limited aggregate of nucleosomes. The double helical cylinder (Woodcock *et al.*, 1984) or the solenoid (Finch and Klug, 1976; Widom and Klug, 1985) are both locally parallel arrangements of stacked nucleosomes. Our own study of diluted chromatin fragments in vitreous water also shows local helical arrangements of stacked nucleosomes (Schultz *et al.*, in preparation).

There is, however, a fundamental difference between the liquid model and previously proposed solid-like models, in which the chromatin is formed by definite stable structures extending over a much larger distance than a nucleosome diameter. This difference can best be illustrated by analogy with another liquid: water. In its usual solid form, each water molecule has four close neighbours at the vertices of a tetrahedron. This geometry defines the ice crystal. The liquid is based on the same tetrahedral structure but each of the tetrahedrons is stochastically distorted in such a way as to prevent the establishment of a long range order and a stable local arrangement (Stillinger, 1980). The characteristic of the liquid is that the disorder is equally distributed over all the molecules. By contrast, the iceberg model which has been used to explain the mobility of the liquid by the free displacement of microcrystalline regions, one with respect to the other, is now generally rejected. In the case of chromosomes where water molecules are replaced by nucleosomes or portions of 11 nm filaments, the iceberg model is analogous to the solid-like models mentioned above, whereas no such stable superstructure exists in the proposed liquid model. A consequence of the liquid model is that local rearrangements, at the level of the nucleosomes or of portions of 11 nm filaments, can take place without long range effects. Another is that self-diffusion, or the inward diffusion of external macromolecules, may take place with vanishingly small force. Such features could be enlightening for understanding the way in which a chromosome performs its function.

Materials and methods

Cell culture and harvesting of metaphase-arrested cells

CHO cells were grown in roller bottles in α-minimum essential medium (α-MEM) supplemented with 10% fetal calf serum, and arrested in metaphase using nocodazole (Sigma) (0.04 μg/ml for 3–6 h) (Zieve *et al.*, 1980). Metaphase-arrested cells were detached by spinning roller bottles at 200 r.p.m. for 4 min, and pelleted at 200 *g* for 10 min at 4°C. HeLa cells were grown and blocked in metaphase using colcemid according to Lewis and Laemmli (1982).

Cryo-preparation

The addition of cyroprotectant was necessary to achieve vitrification of all samples used for sectioning. For whole cells, 20% sucrose (w/v) was incorporated into α-MEM. Samples were pelleted in cryoprotectant in a Beckman microfuge for 2 min at 9000 g. In some experiments, whole cells were cyro-protected by adding 30% dextran (500 000 mol. wt) to the medium.

The freezing procedure was similar to that used previously for the study of bacterial pellets (Dubochet *et al.*, 1983; McDowall *et al.*, 1983). Small volumes (10^{-2}–10^{-1} mm^3) of sample were rapidly transferred to the tip of a metal pin mounted on a plunger, which was immediately propelled into liquid ethane close to its melting point. The cold pin was transferred under liquid nitrogen into the Reichert FC4 (Vienna, Austria) cyromicrotome equipped with a diamond (Diatome, Bienne, Switzerland) or glass knife. Nominal cutting temperature was always below 120 K. Sections were cut manually using a rapid return stroke, and section thickness was typically in the range 100–150 nm. Sections were mounted on cold carbon-coated 600-mesh hexagonal grids (Science Services, Munich) with an eye lash, and flattened by pressing between two cold metal plates, where the sample was kept in liquid nirogen until transfer to the electron microscope.

The specimens were mounted into the cyrospecimen holder PW 6591/100 (Philips, Eindhoven, The Netherlands) under liquid nitrogen, and rapidly inserted into a Philips 400 electron microscope equipped with an improved anti-contaminator (Homo *et al.*, 1984). Observations were made with 80 kV electrons at a specimen temperature of ~120 K, taking care to minimize exposure of the specimen to electrons. Convenient underfocussing was between 2 and 10 μm. Magnification was checked with a cross-grating replica. Micrographs were recorded on Kodak electron image film SO 163 developed for 12 min in D-19, full strength. Mass thickness of the sections was determined from the optical density of the micrograph (Eusemann *et al.*, 1982). Hydration was calculated by comparing the mass thickness of the section before and after freeze-drying (Dubochet *et al.*, 1983).

Conventional plastic embedding

For conventional electron microscopy, whole cells were placed in medium containing 20% sucrose, pelleted and resuspended in a fixative consisting of 2% glutaraldehyde and 4% formaldehyde in 0.1 M Na cacodylate, pH 7.4, containing 20% (w/v) sucrose, and washed in two changes of 0.1 M cacodylate, also containing 20% (w/v) sucrose. Post-fixation was in 1% OsO_4 in 0.1 M Na cacodylate, pH 7.4. Specimens were dehydrated in ethanol, taken through propylene oxide and embedded in Epon. Sections were double-stained with uranyl acetate followed by lead citrate.

Acknowledgements

We are grateful to Dr Carol Featherstone and Alix Cockcroft for help with cell culture. We would like to thank Drs W.Franke and R.Quinlan for valuable discussions, as also Drs M.Renz and Y.Bouligand. We are grateful to M.Adrian and C.Barber for help with the preparation of the manuscript.

References

Adrian,M., Dubochet,J., Lepault,J. and McDowall,A.W. (1984) *Nature*, **308**, 32–36.

Bostock,C.J. and Sumner,A.T. (1978) *The Eukaryotic Chromosome*. North Holland Publishing Co., Amsterdam/NY/Oxford.

Bram,S., Baudy,P., Lepault,J. and Hermann,D. (1977) *Nucleic Acids Res.*, **4**, 2275–2282.

Butler,P.J.G. (1983) *CRC Crit. Rev. Biochem.*, **15**, 57–91.

Chang,J.-J., McDowall,A.W., Lepault,J., Freeman,R., Walter,C.A. and Dubochet,J. (1983) *J. Microsc.*, **132**, 109–123.

Compton,J.L., Hancock,R., Oudet,P. and Chambon,P. (1976) *Eur. J. Biochem.*, **70**, 555–568.

Davies,H.G. and Small,J.V. (1968) *Nature*, **217**, 1122–1125.

Dubochet,J. and Noll,M. (1978) *Science*, **202**, 280–286.

Dubochet,J., McDowall,A.W., Menge,B., Schmid,E.N. and Lickfeld,K.G. (1983) *J. Bacteriol.*, **155**, 381–390.

Dubochet,J., Adrian,M., Schultz,P. and Oudet,P. (1986) *EMBO J.*, **5**, 519–528.

Eusemann,R., Rose,H. and Dubochet,J. (1982) *J. Microsc.*, **128**, 239–249.
Finch,J.T. and Klug,A. (1976) *Proc. Natl. Acad. Sci. USA*, **73**, 1897–1901.
Finch,J.T., Lutter,L.C., Rhodes,D., Brown,R.S., Rushton,B., Levitt,M. and Klug,A. (1977) *Nature*, **269**, 29–36.
Homo,J.-Cl., Booy,F., Labouesse,P., Lepault,J. and Dubochet,J. (1984) *J. Microsc.*, **136**, 337–340.
Jorcano,J.L., Meyer,G., Day,L.A., Renz,M. (1980) *Proc. Natl. Acad. Sci. USA*, **77**, 6443–6447.
Klug,A. and Butler,P.J. 61983) *Horizons Biochem. Biophys.*, **7**, 1–41.
Langmore,J.P. and Paulson,J.R. (1983) *J. Cell Biol.*, **96**, 1120–1131.
Langmore,J.P. and Schutt,C. (1980) *Nature*, **288**, 620–622.
Lepault,J. and Pitt,T. (1984) *EMBO J.*, **3**, 101–105.
Lepault,J., Pattus,F. and Martin,N. (1985) *Biochim. Biophys. Acta*, **820**, 315–318.
Lewis,C.D. and Laemmli,U.K. (1982) *Cell*, **29**, 171–181.
McDowall,A.W., Chang,J.-J., Freeman,R., Lepault,J., Walter,C.A. and Dubochet,J. (1983) *J. Microsc.*, **131**, 1–9.
McDowall,A.W., Hofmann,W., Lepault,J., Adrian,M. and Dubochet,J. (1984) *J.Mol. Biol.*, **178**, 105–111.
Paulson,J.R. and Laemmli,U.K. (1977) *Cell*, **12**, 817–828.
Rattner,J.B. and Hamkalo,B.A. (1978) *Chromosoma*, **69**, 363–372.
Stillinger,F.H. (1980) *Science*, **209**, 451–457.
Widom,J. and Klug,A. (1985) *Cell*, **43**, 207–213.
Woodcock,C.L.F., Frado,L.-L.Y. and Rattner,J.B. (1984) *Cell Biol.*, **99**, 42–52.
Zentgraf,H. and Franke,W.W. (1984) *J. Cell Biol.*, **99**, 272–286.
Zieve,G.W., Turnbull,D., Mullins,J.M. and McIntosh,J.R. (1980) *Exp. Cell Res.*, **126**, 397–405.

Received on 3 March 1986; revised on 24 March 1986